SIAM J. APPL. MATH.
Vol. 78, No. 5, pp. 2575–2596

© 2018 Society for Industrial and Applied Mathematics

THRESHOLD OF FRONT PROPAGATION IN NEURAL FIELDS: AN INTERFACE DYNAMICS APPROACH

GREGORY FAYE[†] AND ZACHARY P. KILPATRICK[‡]

Abstract. Neural field equations model population dynamics of large-scale networks of neurons. Wave propagation in neural fields is often studied by constructing traveling wave solutions in the wave coordinate frame. Nonequilibrium dynamics are more challenging to study, due to the nonlinearity and nonlocality of neural fields, whose interactions are described by the kernel of an integral term. Here, we leverage interface methods to describe the threshold of wave initiation away from equilibrium. In particular, we focus on traveling front initiation in an excitatory neural field. In a neural field with a Heaviside firing rate, neural activity can be described by the dynamics of the interfaces, where the neural activity is at the firing threshold. This allows us to derive conditions for the portion of the neural field that must be activated for traveling fronts to be initiated. Explicit equations are possible for a single active (superthreshold) region and special cases of multiple disconnected active regions. The dynamic spreading speed of the excited region can also be approximated asymptotically. We also discuss extensions to the problem of finding the critical spatiotemporal input needed to initiate waves.

Key words. neural field equations, traveling fronts, propagation threshold, interface equations

AMS subject classifications. 92C20, 35R09

DOI. 10.1137/18M1165797

1. Introduction.

Traveling waves are ubiquitous in nature, arising in a wide variety of biological processes, including epidemics [26], actin polymerization [1], and evolution [38]. These processes are usually modeled by nonlinear partial differential equations (PDEs) that combine nonlinear local interactions and spatial dynamics like diffusion [35]. Such continuum equations can yield traveling wave solutions in closed form, so the effect of model parameters on wave dynamics can be quantified in detail. For instance, neural field models describe large-scale dynamics of nonlocally connected networks of neurons, and their constituent functions can be tuned to produce a multitude of spatiotemporal solutions [7]. Such results can be connected to coherent neural activity patterns observed in cortical slice and in vivo experiments [28, 29, 37].

Large-scale neural activity imaged using voltage sensitive dye exhibits myriad forms of propagating neural activity in different regions of the brain [41, 43]. For instance, sensory inputs can nucleate traveling waves in olfactory [16] and visual cortices [27]. Waves may propagate radially outward from the site of nucleation [23], with constant direction as plane waves [44], or rotationally as spiral waves [29]. Sufficiently large amplitude sensory stimuli can initiate traveling waves of neural activity, but the threshold for initiation is difficult to identify [39]. A recent study has shown that if two visual stimuli are presented sufficiently close together in time, only a single wave is generated [25]. This suggests there is an internal state-der3014ring thres(t)-27856 Td [s013H2h-370(4u)1(21(o)1(n)-442(

consequence, throughout the manuscript we assume $\in (0, 1/2)$. We derive this con-

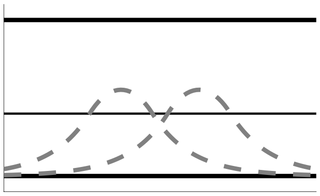

Fig. 1. *Long term behavior of initial conditions* $u_0(x)$ *for* (1) *in one dimension.* (A) *Entirely subthreshold (superthreshold) initial conditions decay (grow). If* $u_0(x) <$ *for all* x*, then* $u\ !\ 0$ *as* $t\ !\ 1$ $(u_<)$*, whereas if* $u_0(x)$ *for all* x*, then* $u\ !\ 1$ *as* $t\ !\ 1$*.* (B) *Initial conditions below (above) the unstable bump* $U_b(x)$ *decay (grow). If* $u_0(x) < U_b(x)$ *for all* x*, then* $u\ !\ 0$ *as* $t\ !\ 1$ $(u_<)$*, whereas if* $u_0(x) > U_b(x)$ *for all* x*, then* $u\ !\ 1$ *as* $t\ !\ 1$*.* (C) *Characterization of* $\lim_{t\ !\ 1} u(x;t)$ *is less straightforward for multimodal initial conditions. Even though each active region* (A_1 *and* A_2*, where* $u_0(x)$) *is narrower than the unstable bump* $U_b(x)$*, this initial condition could lead to propagation due to nonlocal interactions.*

characterized in detail in previous works, so we will simply state key formulas rather than carrying out derivations [2, 5, 7, 9, 11, 18, 24, 32].

2.1. Bump solution. Stationary bumps $u(x;t) = U_b(x)$, with a single active region $U_b(x)$ for $x\ 2\ [x_1;x_2]$, centered at $x = 0$, so $x\ 2\ [\ b;b]$ take the form

$$U_b(x) = \int_{b}^{b} w(x \quad y)\mathrm{d}y = W(x+b) \quad W(x \quad b); \tag{3}$$

where we have defined the antiderivative of the weight kernel

$$W(x) = \int_0^x w(y)\mathrm{d}y: \tag{4}$$

The threshold condition $U_b(\ b) = W(2b) =$ can be solved to identify the unique bump half-width b: $b_0(\ ) = W^{\ 1}(\ )=2$ for any $\ 2\ (0;1=2)$. Local stability analysis can be used to show U_b is linearly unstable [2, 24].

2.2. Periodic solutions. There are also L-periodic stationary solutions $U_L(x)$ with an infinite number of superthreshold regions $[_{n=\ 1}^{1}[\ b+nL;b+nL]$, under the restriction $2b < L$, which take the form [32]

$$U_L(x) = \sum_{n2\mathbb{Z}} \int_{b+nL}^{b+nL} w(x \quad y)\mathrm{d}y = \sum_{n2\mathbb{Z}} (W(x+b+nL) \quad W(x \quad b+nL)): \tag{5}$$

Applying any threshold condition, $U_L(\ b+nL) =$, we obtain an implicit equation)a()))]TJ/F11 9.94].

Since $W_{1} = 1{=}2$, (10) will only have a solution with corresponding $c\ 2\ (0;1)$ if $2\ (0;1{=}2)$, since the integral on the left-hand side is positive and bounded from above by W_{1}. Local stability has been studied previously [13], demonstrating the wave solution U_f is marginally stable to perturbations that shift its location.

This concludes our analysis of entire solutions to (1) in the case $I\ \ 0$. Guided by the fact that the homogeneous solutions $u\ \ 0;1$ are stable, and the intermediate bump $U_b(x)$ and periodic solutions $U_L(x)$ are unstable, we generally expect initial conditions $u_0(x)$ to either be attracted to $u\ \ 0$ or $u\ \ 1$ as $t\ !\ 1$. In the next section, we demonstrate a means of determining the fate of unimodal initial conditions using interface equations.

3. Nonequilibrium dynamics of a single active region.

In this section, we identify conditions on $u_0(x)$ with a single active region ($u_0(x)\ \ \ $ for $x\ 2\ [x_1;x_2]$), so the solution to (1) propagates (assuming $I(x;t)\ \ 0$). In what follows, we assume $0\ \ u_0(x)\ \ 1$ is unimodal, $u_0^0(x_0) = 0$, and $u_0^0(x)\ ?\ 0$ for $x\ 7\ x_0$, ensuring there are no more than two interfaces for $t > 0$. First, we derive results for even $u_0(x) = u_0(\ x)$, and then we extend to asymmetric $u_0(x)$. Initial conditions can be separated into subthreshold ones that lead to decay and superthreshold ones that lead to propagation. Lastly, we identify conditions on the external input $I(x;t)$ to (1) that ensure propagation when $u_0(x)\ \ 0$.

3.1. Interface equations and criticality: Even symmetric case.

Symmetry of (1) with $I\ \ 0$ ensures solutions with even initial conditions are always even, so the active region $A(t) = fx\ 2\ \mathrm{R}\ j\ u(x;t)\ \ \ g$ is symmetric for $t > 0$. The dynamics of the symmetric active region $A(t) = [\ a(t);a(t)]$ can be described with interface equations for the two points $x = \ a(t)$ (see [2, 15]). We start by rewriting (1) as

$$@_t u(x;t) = \ u(x;t) + \mathrm{Z}_{A(t)} w(x\ \ y)\mathrm{d}y; \tag{11}$$

which can be further simplified:

$$@_t u(x;t) = \ u(x;t) + W(x + a(t))\ \ W(x\ \ a(t)):$$

Equation (11) remains well defined even in the case where $a(t)$ vanishes. We can describe the dynamics of the two interfaces by the implicit equations

$$u(\ a(t);t) = \ : \tag{12}$$

Differentiating (12) with respect to t, we find the total derivative is

$$(t)a^0(t) + @_t u(\ a(t);t) = 0; \tag{13}$$

where we define $a^0(t) = \frac{\mathrm{d}a(t)}{\mathrm{d}t}$ and $\ (t) = @_x u(\ a(t);t)$. The symmetry of (13) allows us to reduce to a single differential equation for the dynamics of $a(t)$:

$$a^0(t) = \ \frac{1}{(t)}[W(2a(t))\ \ \ ]; \tag{14}$$

where we have substituted (11) at $a(t)$ for $@_t u(a(t);t)$. Equation (14) is not well-defined t); t W(x+ a(t) for @]x y)d fell08826 Tfl dely which we can integrate and evaluate at $a(t)$ to find

$$(15) \qquad (t) = u_0^0(a(t))\mathrm{e}^{\quad t} + \mathrm{e}^{\quad t}\int_0^t \mathrm{e}^s\,[w(a(t) + a(s)) \quad w(a(t) \quad a(s))]\,\mathrm{d}s:$$

Thus, we have a closed system describing the evolution of the right interface $a(t)$ of the active region $A(t)$, given by (14) and (15), along with the initial conditions $a(0) = `$ and $(0) = u_0^0(`) <$

dynamics, (14) and (15), breaks down. We know this because $W(2a(t)) - \theta < 0$ and decreases as $a(t)$ decreases. Note also that for $t \in (0, t_0)$ we consistently have $\alpha(t) < 0$. Inspecting (15) shows that $\lim_{t \to t_0} \alpha(t) = 0$ since $u_0'(0) = 0$. Thus, at time $t = t_0$, we have $0 \leq u(x, t_0) \leq \theta$, and for $t \geq t_0$, $\partial_t u(x, t) = -u(x, t)$, so $u(x, t) = e^{t_0 - t} u(x, t_0)$ for $t \geq t_0$, and $\lim_{t \to \infty} u(x, t) \equiv 0$, uniformly on $x \in \mathbb{R}$ (Figure 3B).

Stagnation. If $\ell = W^{-1}(\theta)/2 =: b_0$, then $a'(t) = 0$ for all time assuming $\alpha(t) < 0$, implying $a(t) \equiv b_0$. Plugging into (15) yields $\alpha(t)$ with $\alpha(t) = (w(2b_0) - w(0))(1 - e^{-t}) + u_0(b_0)e^{-t} < 0$. As a consequence, $a(t) = b_0$ for all time and $\lim_{t \to \infty} \alpha(t) = w(2b_0) - w(0)$. Furthermore, we can explicitly solve for

$$u(x, t) = W(x + b_0) - W(x - b_0) + e^{-t}[u_0(x) - W(x + b_0) + W(x - b_0)],$$

so $\lim_{t \to \infty} u(x, t) \equiv U_b(x)$, uniformly on $\mathbb{R}$. We call this case stagnation as the active region remains fixed for $t > 0$ (Figure 3C).

To summarize, we have shown the following result.

Starting with smooth unimodal even initial conditions,

$$\lim_{t \to \infty} \ (t) = \lim_{t \to \infty} \Big(u_0'(a(t))e^{\ t} + \int_0^t e^{\ (t\ \ s)}[w(c(t$$

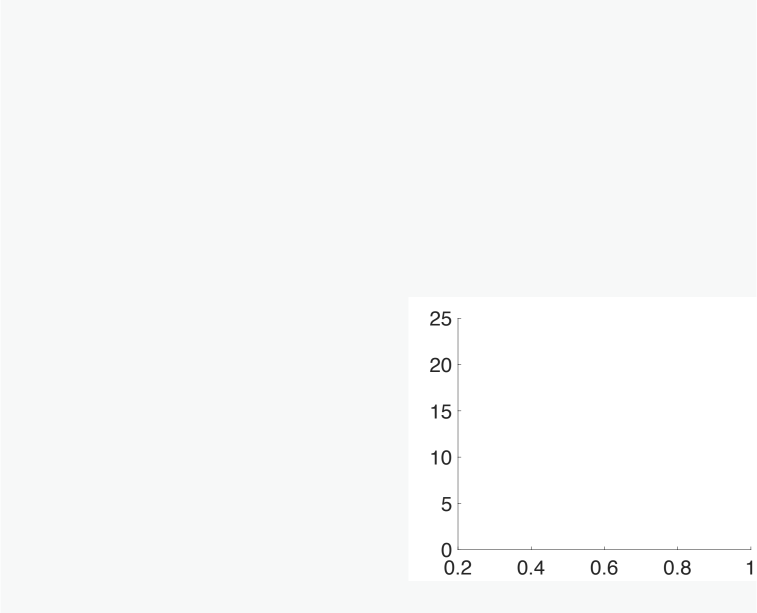

Fig. 5. *Bounds and asymptotics for an exponential kernel,* $w(x) = \mathrm{e}^{\ jxj}=2$. (A) *Propagation occurs if* $` := a(0) > b_0$ *for* $b_0 = \ \ln[1 \quad 2\ ]=2$ *(solid line); extinction occurs if* $` < b_0$. *Numerical simulations (circles) determine* b_0 *by computing* (1) *starting with* $u(x;0) = u_0(x)$ *and identifying* b_0 *for which stagnation occurs* ($u_0(b_0) = \quad$). *Results are consistent whether choosing* $u_0(x) = U \quad U_b(x); U\mathrm{e}$

4. Multiple active regions. We now turn our attention to the more general case of multimodal initial conditions. Since this can now lead to multiple disjoint active regions (where $u_0(x) \geq \theta$), we must extend our analysis from section 3 to track more than two interfaces (see also [33]). While it is difficult to analyze the resulting system of equations explicitly, we can gain insight by focusing on two specific cases of $u_0(x)$: (a) periodic initial conditions with an infinite number of active regions and (b) two symmetric active regions. We begin by deriving the interface equations in the general case.

4.1. Interface equations: General case. When $u_0(x) \geq \theta$ for multiple disjoint active regions, $A(0) = \cup_{j=1}^{N} [a_j(0), b_j(0)]$, the time evolution of $A(t)$ is implicitly described by

$$u(a_j(t), t) = u(b_j(t), t) = \theta, \qquad j = 1, \dots, N, \tag{23}$$

for an initial time $0 < t < t_0$. Differentiating (23) with respect to t, we find

$$\alpha_j(t) a_j'(t) + \partial_t u(a_j(t), t) = 0, \qquad \beta_j(t) b_j'(t) + \partial_t u(b_j(t), t) = 0, \qquad j = 1, \dots, N, \tag{24}$$

where $\alpha_j(t) = \partial_x u(a_j(t), t)$ and $\beta_j(t) = \partial_x u(b_j(t), t)$. Rearranging (24), applying (11) for u_t, and solving for $z = u_x$ as before, we find the following system describing the evolution of the interfaces $(a_j(t), b_j(t))$ and gradients $(\alpha_j(t), \beta_j(t))$:

$$a_j'(t) = -\frac{1}{\alpha_j(t)} \left[\sum_{k=1}^{N} \left(W(b_k(t) - a_j(t)) - W(a_k(t) - a_j(t)) \right) - \theta \right], \tag{25a}$$

$$b_j'(t) = -\frac{1}{\beta_j(t)} \left[\sum_{k=1}^{N} \left(W(b_k(t) - b_j(t)) - W(a_k(t) - b_j(t)) \right) - \theta \right], \tag{25b}$$

$$\alpha_j(t) = e^{-t} \int_0^t e^{s} \sum_{k=1}^{N} \left[w(a_j(t) - a_k(s)) - w(a_j(t) - b_k(s)) \right] ds + u_0'(a_j(t)) e^{-t}, \tag{25c}$$

$$\beta_j(t) = e^{-t} \int_0^t e^{s} \sum_{k=1}^{N} \left[w(b_j(t) - a_k(s)) - w(b_j(t) - b_k(s)) \right] ds + u_0'(b_j(t)) e^{-t} \tag{25d}$$

for $j = 1, \dots, N$. The initial conditions $u_0(a_j(0)) = u_0(b_j(0)) = \theta$ close the system. We expect $\alpha_j(t) \geq 0$ and $\beta_j(t) \leq 0$, since they are at the left and right boundaries of each active region. For the system (25), there is no straightforward condition that

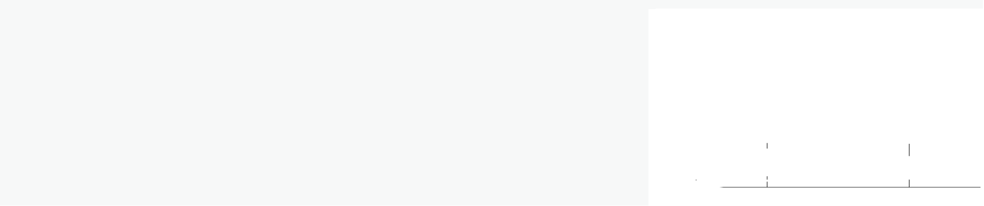

Fig. 6. *Long term behavior of $u(x;t)$, given a periodic initial condition with $u_L(\pm\ell_L + nL) = \kappa$ for all $n \in \mathbb{Z}$, depends on the relation between ℓ_L and $b_L = \mathcal{W}_L^{-1}(\kappa)$. (A) If $\ell_L > b_L$, saturation occurs, and $\lim_{t\to\infty} u(x;t) \equiv 1$. (B) If $\ell_L < b_L$, extinction occurs, and $\lim_{t\to\infty} u(x;t) \equiv 0$. (C) If $\ell_L = b_L$, stagnation occurs, and $\lim_{t\to\infty} u(x;t) = U_L(x)$ as in* (5).

periodic. For an even and periodic initial condition $u(x;0) = u_L(x)$ of period L, $A(t) = \cup_{n\in\mathbb{Z}}[-a(t)+nL; a(t)+nL]$, so by symmetry we can reduce (25) to

$$a'(t) = \frac{1}{\alpha(t)}[\mathcal{W}_L(a(t)) - \kappa]; \tag{26a}$$

$$\alpha(t) = u_L'(a(t))e^{-t} + e^{-t}\int_0^t e^s \sum_{n\in\mathbb{Z}} w_n(a(t);a(s))ds; \tag{26b}$$

where $w_n(a(t);a(s)) = w(a(t)+a(s)+nL) - w(a(t)-a(s)+nL)$ and $\mathcal{W}_L(x)$ is defined as in (6). Fixing L, the initial condition $u_L(x)$ is defined by the single parameter $\ell_L := a(0)$, where $u_L(\pm\ell_L + nL) = \kappa$ for all $n \in \mathbb{Z}$. Criticality occurs for $\ell_L = b_L(\kappa) = \mathcal{W}_L^{-1}(\kappa)$, the half-width of each active region of the periodic solution $U_L(x)$ to (5). The analysis proceeds along similar lines to that given in section 3.1 for the single active region case yielding the following results (illustrated in Figure 6):

Starting with smooth L-periodic, even initial conditions, $u_L(x)$, unimodal on $[-L/2; L/2]$, the fate of the solutions $u(x;t)$ to (1) *falls into three cases:*

(i) *If $\ell_L > \mathcal{W}_L^{-1}(\kappa)$, then $u \to 1$ uniformly on $\mathbb{R}$ as $t \to +\infty$;*

(ii) *if $\ell_L < \mathcal{W}_L^{-1}(\kappa)$, then $u \to 0$ uniformly on $\mathbb{R}$ as $t \to +\infty$;*

(iii) *if $\ell = \mathcal{W}_L^{-1}(\kappa)$, then $u \to U_L$ uniformly on $\mathbb{R}$ as $t \to +\infty$.*

Asymptotic results. Similar to the single active region case, we can obtain leading order approximations for the transient dynamics approaching the homogeneous states. For periodic initial conditions, we do not obtain traveling waves in the long time limit. In the case of saturation, we can estimate the time t_0 at which $u(x;t_0) \approx \kappa$, assuming $L/2 - a(t)$, $\alpha(t)$, and t_0 are small. We approximate $\alpha(t) \approx u_L''(L/2)(\ell_L - L/2)$, so $t_0 \approx (L - 2\ell_L)^2 u_L''(L/2)/[2 - 4\kappa]$.

In the case of extinction, the calculation is quite similar to that presented in section 3.3, and we find $u(x;t_0) \approx \kappa$ at $t_0 \approx \ell_L^2|u_L''(0)|/\kappa$ in the limit $0 < \ell_L \ll 1$.

Exponential kernels. Assuming $w(x)$ is given by (2), we can obtain a simple implicit expression for the critical half-width $b_L := \mathcal{W}_L^{-1}(\kappa)$. Plugging (2) into (6), we can simplify the threshold condition $U_L(\pm b + nL) = \kappa$ to the form [32]

$$\kappa = \frac{\sinh(b)}{\sinh(L/2)}\cosh(L/2 - b) := \mathcal{W}_L(b). \tag{27}$$

Equation (27) must be solved numerically (Figure 7A), showing b_L increases with κ and L. The formula for U_L can also be reduced to yield

Fig. 7. *Stationary periodic solutions* U_L *to* (1) *with exponential kernel,* (2). (A) *Half-width* b_L *of the active region on each period* L *increases with threshold and period* L, *as determined by* (27). (B) *Increasing* L *yields periodic patterns (corresponding to dots in panel A at*

(27*.931Tf 7.986 0 T05580 Td [(.)]TJ/F25 7.9701 Tf 74388 0 Td

The system (29) is closed by the initial conditions $a(0) = \ell_1$ and $b(0) = \ell_2$. As opposed to the single active region case, it is not possible to develop a simple condition on $(\ell_1;\ell_2)$ that determines whether propagation, extinction, or stagnation occurs in the long time limit. However, we can still partition the space of initial conditions $(\ell_1;\ell_2)$ into several cases, for which the long term behavior of (1) is determined by the initial transient dynamics of $(a(t);b(t))$. Observe that both $W(b(t)+a(t)) \quad W(2a(t)) > 0$ and $W(2b(t)) \quad W(b(t)+a(t)) > 0$ for all time whenever they are well defined (i.e., as long as $0 < a(t) < b(t)$). As a consequence, we can already rule out the trivial case where $\ell_2 \quad \ell_1 \quad W^{\ 1}(\ )$.

Class I: $\boldsymbol{\ell_2 \quad \ell_1 \quad W^{-1}(\ )}$**.** In this case, we automatically deduce that $b'(t) > 0$ while $a'(t) < 0$ for all time where they are both well defined. This implies that there exists a finite $t \ > 0$ at which we have $a(t\ ) = 0$. At this point, the two active regions merge to form a single active region given at time $t = t$ by $[\ b(t\ );b(t\ )]$ with $2b(t\ ) > 2\ell_2 > W^{\ 1}(\ )$ as $\ell_2 \quad \ell_1 \quad W^{\ 1}(\ )$. As a consequence, we are back to the propagation scenario studied in section 3.1, and we find the associated solution of the neural field equation (1) obeys $u \to 1$ locally uniformly on $x \in \mathbb{R}$ as $t \to +\infty$.

Class II. $\boldsymbol{\ell_2 \quad \ell_1 < W^{-1}(\ )}$**.** We now discuss the case where $\ell_2 \quad \ell_1 < W^{\ 1}(\ )$. In order to simplify the presentation, we define the following two quantities:

$$W_1(\ell_1;\ell_2) := W(\ell_2 \quad \ell_1) \qquad + W(\ell_1+\ell_2) \quad W(2\ell_1);$$
$$W_2(\ell_1;\ell_2) := W(\ell_2 \quad \ell_1) \qquad + W(2\ell_2) \quad W(\ell_1+\ell_2);$$

defined for all $0 < \ell_1 < \ell_2$. It is crucial to observe that $W_1(\ell_1;\ell_2) \quad W_2(\ell_1;\ell_2) = 2W(\ell_1+\ell_2)$ 1 9.101 0 Td [(x)]TJ/F1 [illegible]

Fig. 8. *Evolution of interfaces for two sy*[illegible] *bumps having Class* II *initial conditions:* $\ell_2 \quad \ell_1 < W^{-1}(\ )$. *Phase portrait of* (29) *in (a*[illegible]*s shown in the case of an exponential kernel,* (2), $= 0.45$, *and the initial condition* $u_0($[illegible] *We fix* $a(0) = \ell_1 = 1/4$ *and vary* $b(0) = \ell_2$ *from* 0.5 *to* 2.25. *Some initial conditions (re*[illegible]*ead to trajectories (black lines) that propagate, while other initial conditions (blue stars) l*[illegible]*nction. Case* A *(*$W_1(\ell_1, \ell_2) > W_2(\ell_1, \ell_2) \quad 0$*):* $a(t)$ *vanishes in finite time with a final* [illegible]*ve the nullcline* $W_2(\ell_1, \ell_2) = 0$ *(where red line meets* ℓ_2 *axis), leading to propagation.* [illegible]*esponding example evolution of* $u(x, t)$. *Case* B *(*$0 \quad W_1(\ell_1, \ell_2) > W_2(\ell_1, \ell_2)$*):* $a(t)$ *a*[illegible]*erge in finite time, leading to extinction. Case* C *(*$W_1(\ell_1, \ell_2) > 0 > W_2(\ell_1, \ell_2)$*): Thre*[illegible]*s are described in the main text, leading to either extinction for subcases* (1) *and* (3) *or pr*[illegible] *for subcase* (2). *Green arrows indicate the direction of the vector field in each subregion. O*[illegible]*s demonstrate behavior of the full neural field model,* (1), *in the cases* A, B, C1, C2, *and* C[illegible]

$= 0$ while $0 > W_2(a(t_1), b(t_1))$; [illegible] case we are back to Case B and extinction occurs.

We illustrate these different [illegible]s on a specific example in Figure 8 using an exponential kernel, (2), and the [illegible]ondition

(30) $$u_0(x) = [illegible] e^{-|x+x_0|} + e^{-|x-x_0|} \Big);$$

which allows us to specify

$$x_0 = \frac{1}{2} \ln \Big(1 + 2\cosh(\ell_1 [illegible] \quad [illegible]d \quad U_0 = \frac{\sqrt{1 + 2\cosh(\ell_1) e^{\ell_2}}}{\cosh(\ell_1)}$$

and ensure that $u_0(\ \ell_{1,2}) =$ [illegible]

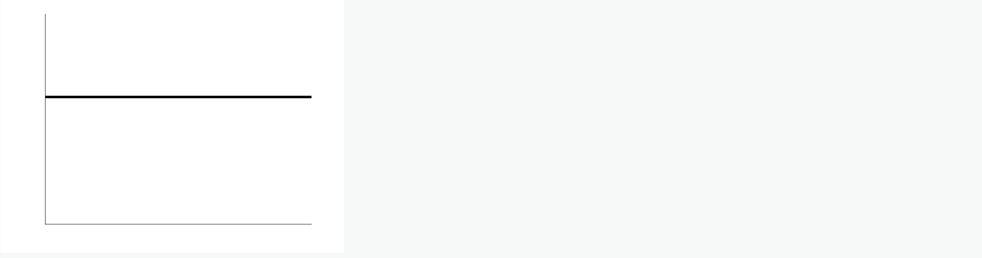

Fig. 9. *Conditions for propagation driven by a spatially periodic input* $I(x;t) = I(x)$ $_{[0;t_1]}$ *with* $I(x) = I(x+L)$ *and* $u(x;0)$ 0. (A) *For periodic, even, and positive profile* $I(x)$ *with* $I(0) >$, *propagation only occurs if* $G_L(b) = \mathbf{W}_L(b) + I(b) =$ *has no solutions. If solutions to* (31) *exist, the minimal one is linearly* (b_s) *or marginally* (b_m) *stable. For inputs* $I(x)$ *that are monotone decreasing on* x 2 $(0;L=2)$, *there are only two solutions.* (B) *If* $G_L(b_s) =$ *is satisfied for some* b_s, $u(x;t_1)$ $U_{L_s}(x)$ *for large* t_1 *with active region centered at* $x = 0$ *given* $[\ a_s;a_s]$, *where* $a_s < b_L$, *so* $\lim_{t\,!\,1} u(x;t)$ 0. (C) *Here* $I(x)$ *is chosen so that* $G_L(b) =$ *has no solutions. If* $t_1 := t_e$, *then* $u_e(\ a_e) := u(\ a_e;t_e) =$ *and* $a_e < b_L$, *so* $\lim_{t\,!\,1} u(x;t)$ 0. *However, for* $t_1 := t_p$ *with* $u_p(\ a_p) := u(\ a_p;t_e) =$ *and* $a_p > b_L$, $\lim_{t\,!\,1} u(x;t)$ 1.

We now discuss the three remaining cases: (I) equation (31) has at least one solution, so saturation does not occur; (II) equation (31) has no solutions, but $_1$ $_c$, the time at which $a(\ _c) = b_L$ for $I(x;\ )$ $I(x)$, and saturation does not occur; (III) equation (31) has no solutions, and $_1 >\ _c$, so saturation occurs.

Case I: $\min_{x 2 \mathbb{R}} G(x)$. Here, (31) has at least one solution. Since we have assumed $I(0) >$, this solution $b_{\min}$ is linearly or marginally stable with respect to even and odd perturbations. Equation (33) implies $\frac{da}{d} > 0$ for all $<\ _1$, but $\frac{da}{d}$ vanishes at $a = b_{\min}$, so $a(\ ) < b_{\min} < b_0$ for all $<\ _1$. Thus, once $=\ _1$, the dynamics is described by the extinction case from section 4.2, and $\lim_{t\,!\,1} u(x;t)$ 0 (Figure 9B).

Case II: $\min_{x 2 \mathbb{R}} G(x) >$ *and* $_1$ $_c$. Here (31) has no solutions, but $a(\ )$ will not grow large enough for saturation to occur once $I(x;\ ) = 0$, since $_1$ $_c$. We define $_c$ as the critical time when $a(\ _c) = b_L = \mathrm{W}_L^{\ 1}(\ )$, given by the formula

$$\text{(34)} \qquad \mathrm{Z}_{\ 0}^{\ \mathbf{W}_L^{\ 1}(\ )} \frac{da}{\mathrm{W}_L(a) \qquad + I(a)} = \mathrm{Z}_{\ t_0}^{\ t_c} \frac{dt}{\ (t)} := \ _c:$$

By definition, $a(\ _1)$ b_L, so once $=\ _1$, the dynamics is described by either (a) the extinction case in section 4.2 if $_1 <\ _c$, so $\lim_{t\,!\,1} u(x;t)$ 0, or (b) the stagnation case in section 4.2 if $_1 =\ _c$, so $\lim_{t\,!\,1} u(x;t)$ $U_L(x)$ (Figure 9C).

Case III: $\min_{x 2 \mathbb{R}} G(x) >$ *and* $_1 >\ _c$. Requiring $_1 >\ _c$ with (34), we have that $a(\ _1) > b_L$. Thus, after $=\ _1$, the dynamics is described by the saturation case in section 4.2, so $\lim_{t\,!\,1} u(x;t)$ 1 (Figure 9C).

5. Discussion. In this paper, we have studied threshold phenomena of front propagation in the excitatory neural field equation (1) using an interface dynamics approach. Our interface analysis projects the dynamics of the integrodifferential equations to a set of differential equations for the boundaries of the active regions, where the neural activity is superthreshold. The interface equations can be used to categorize initial conditions or external stimuli based on whether the corresponding long term dynamics of the neural field are extinction (u ! 0), propagation/saturation (u ! 1), or stagnation (u ! $U_{\mathrm{stat}}(x)$ 6 $0;1$). We considered several classes of initial conditions, which admit explicit results: (i) functions with a single active region, (ii) even and periodic functions with an infinite number of active regions, and (iii) a two-parameter family of even functions with two active regions. In these particular cases, the conditions for extinction, propagation/saturation, or stagnation can be expressed in terms of a few inequalities for the parameters specifying the initial conditions. We were able to obtain a similar trichotomy when the neural field equation (1) is forced by a fixed critical stimulus (e.g., unimodal and periodic) over a finite time interval. Our analysis assumes the nonlinearity in the neural field arises from a Heaviside firing rate function, so the dynamics of the neural field equation (1) can be equivalently expressed as differential equations for the spatial locations where the neural activity equals the threshold of the firing rate function. This work addresses an important problem in the analysis of models of large-scale neural activity, determining the long term behavior of neuronal network dynamics that begin away from equilibrium.

There are several natural extensions of this work that build on the idea of developing critical thresholds for propagation in neural fields using an interface dynamics approach. For instance, one possibility would be to consider a planar version of (1)

[11]

[41] X.-J. Wang, *Neurophysiological and computational principles of cortical rhythms in cognition*, Physiol. Rev., 90 (2010), pp. 1195{1268.

[42] H. R. Wilson and J. D. Cowan, *A mathematical theory of the functional dynamics of cortical and thalamic nervous tissue*, Biol. Cybernet., 13 (1973), pp. 55{80.

[43] J.-Y. Wu, X. Huang, and C. Zhang, *Propagating waves of activity in the neocortex: What they are, what they do*, Neuroscientist, 14 (2008), pp. 487{502.

[44] W. Xu, X. Huang, K. Takagaki, and J.-Y. Wu, *Compression and reflection of visually evoked cortical waves*, Neuron, 55 (2007), pp. 119{129.

[45] A. Zlatos, *Sharp transition between extinction and propagation of reaction*, J. Amer. Math. Soc., 19 (2006), pp. 251{263.